Microscopic description of isobaric-analog-state transitions induced by 25-, 35-, and 45-MeV protons*

R. R. Doering, D. M. Patterson,† and Aaron Galonsky
Cyclotron Laboratory, Department of Physics, Michigan State University, East Lansing, Michigan 48824

(Received 3 March 1975)

Differential cross sections have been measured for (p,n) reactions to the isobaric analogs of the targets ^{48}Ca, ^{90}Zr, ^{120}Sn, and ^{208}Pb at proton bombarding energies of 25, 35, and 45 MeV. The isospin-flip strength of a phenomenological nucleon-nucleon force has been determined with microscopic distorted-wave calculations including the "knock-on" exchange amplitude. A realistic G-matrix effective interaction also provides a reasonable account of the observed cross sections, particularly at the higher proton energies.

[NUCLEAR REACTIONS ^{48}Ca, ^{90}Zr, ^{120}Sn, ^{208}Pb(p,n), $E=25$, 35, 45 MeV; measured IAS $\sigma(\theta)$; compared with microscopic direct-reaction model; deduced effective nucleon-nucleon interaction. Included knockon exchange amplitude.]

I. INTRODUCTION

Many nuclear-reaction cross sections have been adequately reproduced with simple one-body potential models of the projectile-target interaction. Nevertheless, a more detailed understanding of nuclear processes requires the calculation of scattering in terms of realistic forces between the individual nucleons. Unfortunately, the nuclear many-body problem cannot be solved exactly with presently available mathematical techniques. Furthermore, realistic nucleon-nucleon potentials are generally too strong for direct perturbation expansions to converge rapidly, if at all. However, approximations based on the multiple-scattering formalism[1] have been employed with reasonable success in both bound-state[2] and scattering[3] calculations.

The multiple-scattering approach to nuclear reactions allows the potential between the projectile and ith target nucleon (v_{ip}) to be replaced with an effective two-body scattering operator which is less pathological. This is accomplished through a rearrangement of the Born series for the scattering amplitude so that the basic interaction includes multiple scattering by a particular target nucleon as the projectile propagates under the average influence of the remainder of the target (the "core"), as represented by a one-body "optical" potential. Such an effective scattering operator may be defined by

$$t_{ip}=v_{ip}+v_{ip}\frac{1}{e^{(+)}}t_{ip}\,, \tag{1}$$

where

$$e^{(\pm)}=E-H_T-k_p-U_{(i)}\pm i\epsilon\,,$$

$$U_{(i)}=\sum_{j(\neq i)=1}^{A}U_j\,,$$

$$(H_T+k_p)\psi=E\psi\,,$$

H_T is the Hamiltonian for the A target nucleons, k_p is the kinetic-energy operator for the projectile, U_j is the contribution of the jth target nucleon to the optical potential, and it is understood that all matrix elements are ultimately evaluated in the limit $\epsilon\to 0$. To first order in t_{ip}, the direct amplitude for inelastic scattering is given by[4]

$$T_{FI}^{(1)}=\sum_{i=1}^{A}\langle\chi_{F(i)}^{(-)}|t_{ip}|\chi_{I(i)}^{(+)}\rangle\,, \tag{2}$$

where

$$\chi_J^{(\pm)}=\psi_J+\frac{1}{e^{(\pm)}}U_{(i)}\psi_J\,,\quad J=I \text{ or } F$$

with initial and final states labeled by I and F, respectively.

Equation (2) has been designated the single inelastic scattering approximation[5] (SISA), since it neglects virtual excitation of the core in intermediate states. Disregarding such processes is an essential feature of the usual microscopic direct-interaction concept of nuclear reactions.[6] However, core excitations are obviously important for a reaction known to proceed through a metastable compound nucleus. Thus, the SISA may only be expected to give a reasonable account of reactions induced by projectiles which bring sufficient energy into the compound nucleus so that the probability of its decay to any particular final state is small compared to that for the competing direct-reaction process. For nucleon-nucleus

elastic scattering, the compound-nucleus reaction mechanism appears to be relatively unimportant for bombarding energies above about 10 MeV.[7]

Given a projectile energy sufficient for the validity of the SISA, one is still faced with solving a many-body problem, represented by Eq. (1), to obtain the effective interaction. At bombarding energies large compared to the optical potential and the energies of the target nucleons, Eq. (1) approaches

$$t_{ip}^{f} = v_{ip} + v_{ip}\frac{1}{E - k_i - k_p + i\epsilon}t_{ip}^{f} \tag{3}$$

which is just the free nucleon-nucleon scattering operator. Using the free interaction in Eq. (2) results in the impulse approximation, which has been demonstrated to be useful for nucleon-nucleus scattering at energies greater than about 100 MeV.[8] At lower energies, the effective scattering of a pair of nucleons is influenced to a greater extent by the proximity of others. This subject has been studied extensively in relation to the nuclear-structure problem,[9] and it has been suggested that the effective interactions used in structure calculations may also be appropriate for medium-energy nucleon-nucleus scattering.[10] It seems plausible that a bound target nucleon should not interact much differently with its neighbors than with a projectile nucleon possessing a kinetic energy only a few tens of MeV greater. Indeed, the bound-state G-matrix effective interaction may be obtained from Eq. (1) by replacing the complex optical potential and the interactions in H_T with a real independent-particle potential, including the Pauli projection operator in the propagator, and deleting the $i\epsilon$.[11] The most significant difference is probably the lack of an imaginary term in the bound-state case. Nevertheless, G-matrix interactions have provided reasonable descriptions of nucleon inelastic scattering[10,12] and the real part of the proton-nucleus optical potential.[13]

The χ's in Eq. (2) contain the initial and final states of the target in addition to the optical wave functions for the relative projectile-target coordinate, which are commonly referred to as the distorted waves. Thus, the scattering amplitude depends on the bound states of H_T, as well as the effective nucleon-nucleon interaction. Therefore, the extent to which the latter is well established determines the amount of nuclear-structure information which may be obtained from nucleon-nucleus scattering experiments. Unfortunately, as has been previously indicated, the calculation of a realistic effective interaction, even with a free nucleon-nucleon potential given, is a formidable undertaking. Furthermore, it is difficult to estimate the effects of the approximations used to calculate interactions on the structure information extracted with them. Thus, it has been proposed that phenomenological effective interactions should be determined from scattering experiments involving nuclei with relatively well-understood structure, so that a "calibrated spectrometer" would be available for investigating more obscure nuclear wave functions.[14]

In general, direct nuclear reactions with large cross sections proceed predominantly via the central-force part of the nucleon-nucleon interaction, the standard phenomenological form of which is given by

$$t_{ip} = V_0 g_0(r_{ip}) + V_\sigma g_\sigma(r_{ip})\vec{\sigma}_i \cdot \vec{\sigma}_p + V_\tau g_\tau(r_{ip}) \times \vec{\tau}_i \cdot \vec{\tau}_p + V_{\sigma\tau} g_{\sigma\tau}(r_{ip})\vec{\sigma}_i \cdot \vec{\sigma}_p \vec{\tau}_i \cdot \vec{\tau}_p , \tag{4}$$

which is a local parametrization of the effective scattering operator, patterned after the corresponding terms in the general two-body potential.[6] For simplicity, a common radial function of either Gaussian or Yukawa form is usually selected. Attempts to extract the associated empirical strengths from nucleon-nucleus scattering data have been reviewed by Austin.[15] Assuming a Yukawa radial dependence with a range of 1.0 fm, he concludes that $V_0 = -27 \pm 5$ MeV, $V_{\sigma\tau} = 12 \pm 2\frac{1}{2}$ MeV, and that V_σ and V_τ are poorly determined. In particular, his compilation includes values of V_τ from below 10 to nearly 30 MeV.

The present study concentrates on obtaining more precise knowledge of the purely isospin-flip part of the effective nucleon-nucleon interaction, which corresponds to the third term in Eq. (4). Since this is the only central-force component which contributes to the direct charge-exchange amplitude between 0^+ isobaric-analog states (IAS),[6] such transitions are quite sensitive to V_τ. Except for the smallness of the cross sections typically observed, (^{3}He, t) reactions are the most experimentally convenient means of studying such charge-exchange transitions. Unfortunately, conventional direct-reaction calculations have often been in relatively poor agreement with the (^{3}He, t) data.[16] Besides the usual optical-model ambiguities for complex projectiles, complications of the reaction mechanism have been proposed. In particular, a (^{3}He, α)(α, t) amplitude larger than the direct amplitude has been calculated for the ^{48}Ca(^{3}He, t)^{48}Sc (IAS) reaction at 23 MeV.[17] Generally accepted optical-model potentials are available for nucleon projectiles, but it has been suggested that neutron pickup followed by proton stripping may also interfere significantly with the direct amplitude for the (p, n) charge-exchange reaction.[18] This is certainly possible if the direct amplitude is considered to represent only the exchange of a charged meson.

However, the multiple-scattering formalism adopted in the present paper introduces an effective scattering operator [Eq. (1)] which represents the complete interaction between the projectile and a particular target nucleon in the presence of the core.[4] Thus, the direct amplitude defined by Eq. (2) already includes the two-step $(p,d)(d,n)$ process. The pseudopotential model [Eq. (4)], however, neglects any nonlocality of the effective interaction, an aspect of multistep mechanisms which allows violations of the usual direct-reaction selection rules governing the transfer of spin and orbital angular momentum.[6] Therefore, two-step effects are most noticeable for relatively weak transitions such as $(^3\mathrm{He},t)$ reactions to 0^+ antianalog states, for which $L=1$ contributions have been observed to overshadow the inhibited $L=0$ amplitudes allowed by local interactions.[19]

For more than a decade, (p,n) IAS experiments have been used to explore the isospin dependence of the nuclear force. However, most of the data have been obtained with proton bombarding energies of less than 30 MeV. The few absolute differential cross sections previously measured with $E_p \geq 30$ MeV are essentially confined to the forward hemisphere and generally have relative errors in excess of 10%.[20-23]

The present work provides (p,n) IAS angular distributions from 0° to 160° at proton energies of 25, 35, and 45 MeV for ^{48}Ca, ^{90}Zr, ^{120}Sn, and ^{208}Pb targets. The ground states (and, hence, the analog states) of these nuclei are 0^+ and considered to be particularly well understood. Thus, these data are especially appropriate for investigating the isospin-flip strength of the effective nucleon-nucleon interaction.

II. EXPERIMENTAL TECHNIQUE

A. Data acquisition

The Michigan State University (MSU) cyclotron provides proton beams of exceptional quality for time-of-flight experiments. Internal slits restrict the phase width of individual beam pulses to approximately 2°. At a typical repetition rate of one pulse every 60 nsec, 2° of phase width corresponds to a time spread of $\frac{1}{3}$ nsec. In practice, γ-ray bursts $\lesssim \frac{1}{2}$ nsec [full width at half-maximum (FWHM)] in duration are observed from thin targets intercepting the external proton beam.

The detector used in this experiment consists of a 7.0-cm-diam by 3.8-cm-thick volume of the liquid scintillator NE 213 encapsulated in a glass cylinder which is coupled by a Lucite light pipe 2.5 cm long to an RCA 8575 photomultiplier tube mounted on an Ortec 270 constant-fraction-timing base. The excellent pulse-shape-discrimination (PSD) properties of NE 213[24] are exploited via the zero-crossing technique[25] to route events induced by incident neutrons and γ rays into separate spectra.

Figure 1 displays superimposed neutron and γ-ray time-of-flight spectra taken at a scattering angle of 0° from a ^{90}Zr target bombarded with 35-MeV protons. Each channel represents 0.1 nsec, and time of flight decreases with increasing channel number as a consequence of providing the time-to-amplitude converter with start signals from the detector and stop signals derived from the zero crossing of the cyclotron rf voltage. In this run, the target γ-ray burst has a duration of 0.39 nsec (FWHM). The time spread of the IAS neutron peak is 60% greater and corresponds to an energy spread of 260 keV (out of 23 MeV) at the 7.22-m flight path. Most of the additional width results from scintillator thickness (165 keV) and target energy loss (110 keV). Less significant contributions to the neutron energy resolution include the energy spread of the incident proton beam and its straggling in the target, which are each less than 50 keV.

The targets employed in this experiment are self-supporting rolled foils. Their thicknesses are approximately 10 mg/cm^2, except for the ^{48}Ca target (1.08 mg/cm^2) and a pair of ^{208}Pb targets (30.0 and 30.2 mg/cm^2) used for the angular distribution at 45 MeV and back angles at 35 MeV. The isotopic enrichments of the ^{48}Ca, ^{90}Zr, ^{120}Sn, and ^{208}Pb targets are 96.25, 98.66, 98.40, and 99.14%, respectively.

The use of relatively thick targets compensates

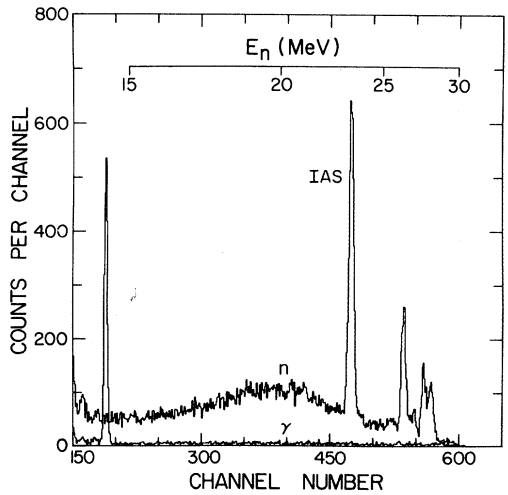

FIG. 1. Neutron (n) and γ-ray (γ) time-of-flight spectra at 0° for 35-MeV protons on ^{90}Zr. Each channel represents 0.1 nsec.

for the inefficiency of the neutron detector by yielding reasonable counting rates with little sacrifice of resolution. The data at each scattering angle have been accumulated during a target bombardment of from 5×10^2 to 1×10^4 μC at a rate between 1 and 4 μA, limited for the tin and lead targets by their low melting points. The spectra in Fig. 1 result from a bombardment of 10^3 μC.

Unfortunately, thick targets also scatter a lot of beam toward potential sources of background. In the present system for taking angular distributions from 10° to 160°, a quadrupole triplet following the target chamber focuses protons scattered through angles less than about 0.022 rad into a heavily shielded beam dump. Unobstructed flight paths at forward scattering angles have been provided by locating the dump shield 7 m beyond the target ladder. To insure adequate measurements of beam intensity, the Faraday cup has been extended from the dump up to the target chamber. Background is further reduced by collimating the detector with a shield of steel and water. The detector and shield ride on a cart which pivots about an axle mounted above the target chamber. The cart floats on a remotely controlled motor-driven air pad.

A special experimental arrangement is available for observing neutrons at a scattering angle of 0°. A magnet following an auxiliary target chamber in the cyclotron vault is used to bend the proton beam about 20° from the 0° neutron flight path. The detector is in a separate vault, shielded from neutrons and γ rays not originating in the target by concrete walls 1.2 m thick. Thus, the 0° spectra also contain little background.

Since only IAS neutrons are of primary interest in the present experiment, a sufficiently high threshold has always been set on the light-pulse-height (LIGHT) signals from the neutron detector to discriminate against low-energy neutrons from a given beam burst which would otherwise overlap with IAS neutrons from the next burst. In most spectra, even the ground state of the residual nucleus has been relatively free from such overlap. For the 3.02- to 7.22-m flight paths currently used, this technique results in higher counting rates for the IAS neutrons than would be obtained through achieving the same dynamic range with lower thresholds by eliminating alternate beam bursts from the cyclotron. An additional advantage of higher thresholds is improved PSD performance, since small-amplitude light pulses from protons and electrons are difficult to distinguish.

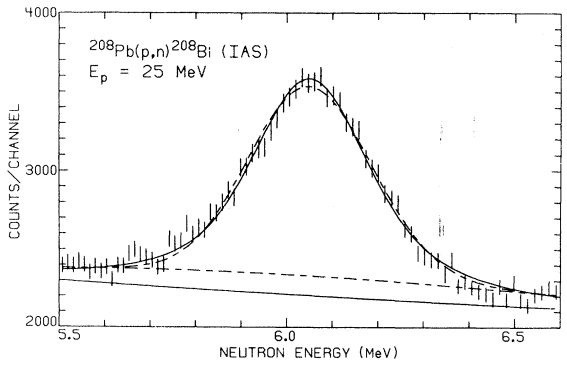

FIG. 2. Neutron spectrum for ^{208}Pb$(p,n)^{208}$Bi at $E_p = 25$ MeV in the region of the isobaric analog of the target ground state. The fits shown are based on Lorentzian (solid) and Gaussian (dashed) intrinsic line shapes plus quadratic backgrounds. The area determined from the Lorentzian search is 50% larger than for the Gaussian.

B. Data reduction

Except for the analog of ^{48}Ca, every IAS observed in this experiment is proton unbound. In such cases, the IAS generally appears as an isolated peak on a smooth continuum. Occasionally, the analogs of excited states of the target are also visible. In particular, the analogs of the lowest 2^+ and 3^- states of ^{90}Zr and ^{120}Sn have been identified in the present data. Analyses of the angular distributions obtained for these states will be published separately.

The computer code ANNIE[26] has been used to calibrate the time-of-flight spectra and to obtain least-squares fits to neutron peaks with a fold of resolution functions representing beam energy spread, target thickness, straggling, kinematic broadening, scintillator thickness, electronic plus beam-burst time spread, and intrinsic state width. The primary need for such a program results from the assumed Lorentzian (Breit-Wigner) intrinsic line shape of the isobaric-analog resonances.[27] The Lorentzian tails are generally indistinguishable from a quadratic background, which can lead to considerably underestimated areas for IAS peaks fitted with less realistic functions. The most significant improvement resulting from the inclusion of a Lorentzian intrinsic line shape in searches on the present data has been obtained for the IAS of ^{208}Pb, since it has the largest natural width. Figure 2 displays a pair of fits for this state. The fit incorporating a Lorentzian intrinsic shape gives 50% more area than its counterpart based on a Gaussian line shape. Total cross sections of 7.1 ± 0.8 and 9.6 ± 1.1 mb have been obtained from IAS peak areas extracted by eye and with ANNIE, respectively, for ^{208}Pb(p,n)-^{208}Bi at 25 MeV.

The principal errors in the present (p, n) IAS cross sections probably reside in the neutron detection efficiencies, which have been calculated with a modified version of Kurz's program TOTEFF.[28] Since the neutron time-of-flight spectra have been gated by a band in the LIGHT-PSD plane encompassing predominantly proton light pulses, only the probabilities for neutron induced reactions producing protons in the scintillator have been summed to yield the total detector efficiency. The relevant nuclear reactions included in TOTEFF are n-p scattering and $^{12}C(n,p)^{12}B$. The probabilities that the reactions will be induced by final-state neutrons from prior $^{12}C(n,n'3\alpha)$ and n-p scattering are also considered. Fortunately, the detection efficiencies calculated for the neutron energies in this experiment result almost exclusively from relatively well determined n-p scattering cross sections. The original n-p angular distributions in TOTEFF have been replaced with values derived from the Yale phase shifts.[29] A few of the carbon reaction cross sections have also been adjusted to agree with recent measurements. The remaining significant differences between the original and MSU versions of TOTEFF involve individual scintillator properties. The scintillator density, hydrogen-carbon ratio, and light response as a function of proton energy have been replaced with appropriate values for NE 213. In particular, the proton light response is currently based on the data of Verbinski *et al.*[30] The LIGHT threshold has been calibrated by fitting the Compton edges of 0.511- to 4.44-MeV γ rays with electron-recoil spectra derived from the Klein-Nishina formula[31] folded with a centrally Gaussian light-resolution function with exponential tails. Since the neutron energy is approximately independent of the scattering angle for these targets, it has been possible to maintain a constant efficiency for each angular distribution by holding a fixed threshold. Thus, errors in the efficiency calculations do not diminish the relative accuracy within each angular distribution.

Another source of errors which affects only the absolute normalization of the present angular distributions is the correction for neutron attenuation along the flight path. In general, the removal cross section is less than the total cross section, since some neutrons may be elastically scattered by potential absorbers into the detector. Some of the absorbers, such as the $\frac{1}{4}$-mm-thick Mylar window on the target chamber and the air along the flight path, are mostly several meters from the detector; neutrons elastically scattered by them at all but very forward angles are attenuated by the collimating shield on the detector cart and delayed by longer flight paths. Thus, the removal cross sections have been equated to the total neutron cross sections for these media. In contrast, neutrons elastically scattered from materials immediately surrounding the scintillator (principally glass and reflectance paint) are not signi-

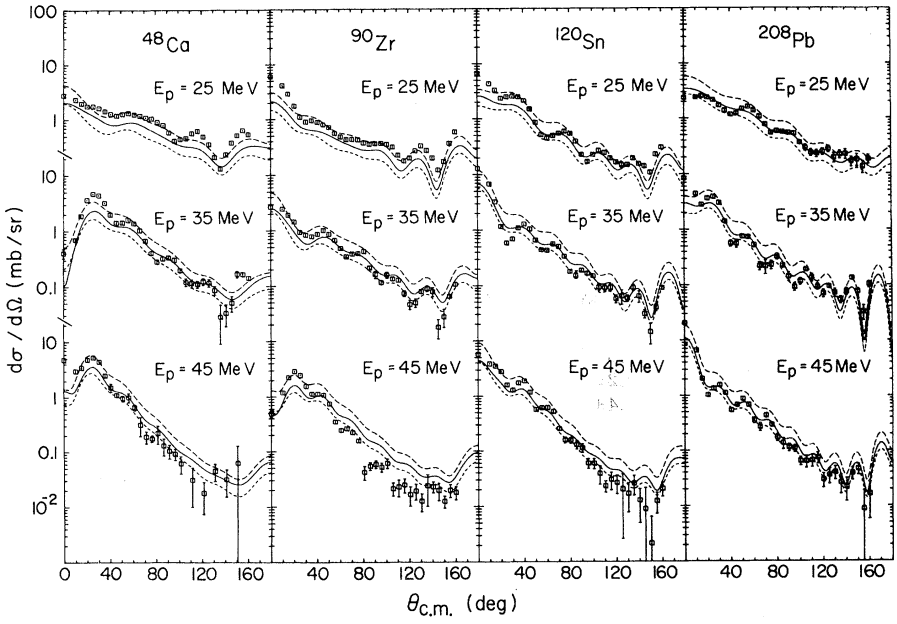

FIG. 3. Comparison of experimental (p, n) IAS angular distributions with microscopic distorted-wave calculations based on phenomenological (dashed) and G-matrix (solid) effective nucleon-nucleon interactions. The short and long dashes correspond to 1.0-fm Yukawa potentials with $V_\tau = 12$ and 18 MeV, respectively.

ficantly attenuated or delayed with respect to those incident directly from the target. Thus, only the nonelastic neutron cross sections have been included for these absorbers. Attenuation corrections ranging from 5% to 20% have been applied to the individual angular distributions.

A NaI(Tl) scintillation counter has been used to monitor protons scattered through 90°. The ratio of observed protons to the product of beam charge and target thickness has remained sufficiently constant throughout each angular distribution so that monitor corrections have not been included.

The error bars displayed on the data in Fig. 3 represent relative errors within each angular distribution which result from statistical uncertainties in the peak fitting combined independently with ±2% fluctuations in the product of beam charge and target thickness. Since the IAS peak area is a search parameter, its variance is the corresponding diagonal element of an error matrix obtained from inverting the curvature matrix determined by the fitting algorithm.[32]

The errors in the absolute magnitudes of the cross sections due to uncertainties in the neutron detection efficiency calculations are estimated to be about 10%.[28,36] There are also small uncertainties in target thickness, beam current integration, and neutron attenuation along the flight path, which introduce systematic errors estimated to be less than 5%. ANNIE has been used to evaluate the additional systematic errors arising from uncertainties in the IAS intrinsic widths. The widths employed in the searches for the IAS yields are 20± 10,[33] 30± 5,[34] and 231± 6 keV[35] for the analogs of ^{90}Zr, ^{120}Sn, and ^{208}Pb, respectively.

TABLE I. (p,n) IAS total cross sections measured in this work.

Target	E_p (MeV)	σ_T (mb)
^{48}Ca	25	10.6± 1.2
	35	10.2± 1.1
	45	8.4± 1.0
^{90}Zr	25	6.7± 0.8
	35	4.8± 0.5
	45	4.4± 0.5
^{120}Sn	25	8.5± 1.0
	35	5.6± 0.6
	45	5.8± 0.7
^{208}Pb	25	9.6± 1.1
	35	6.8± 0.8
	45	5.4± 0.6

The individual angular distributions have been integrated to yield the total cross sections listed in Table I. The corresponding errors have been obtained by combining the aforementioned statistical and systematic errors independently. Tabulations of the differential cross sections and their relative errors are available upon request.

III. ANALYSIS

A. Microscopic calculations

Except for the presence of an effective scattering operator rather than the free two-body potential, the direct SISA amplitude [Eq. (2)] is equivalent to the corresponding amplitude in the distorted-wave Born approximation (DWBA).[37] Thus, if the effective interaction defined by Eq. (1) is represented by a local pseudopotential [e.g., Eq. (4)], conventional DWBA programs may be used to compute the cross sections.

The theoretical angular distributions in Fig. 3 have been calculated with the code DWBA70,[38] which incorporates the helicity representation[39] and evaluates the knock-on exchange amplitude without resorting to a local approximation.[10] The knock-on amplitude is the principal effect of antisymmetrization for inelastic scattering[6] and may be derived consistently within the framework of multiple-scattering theory.[40] DWBA70 is applicable to reactions in which the state of the residual nucleus may be expressed as a sum of particle-hole pairs with respect to the target ground state. Thus, the scattering amplitude is decomposed into a series of terms each representing the creation of a particular pair with a spectroscopic amplitude[41] defined by

$$Z_J(n_p, n_h) = (2J+1)^{-1/2}(2J_I+1)^{-1/2} \times \langle \Phi_F | A_J^\dagger(n_p, n_h) | \Phi_I \rangle , \quad (5)$$

where J is the total angular momentum transferred, J_I is the spin of the target, the Φ's are eigenstates of H_T, and $A_J^\dagger(n_p, n_h)$ is the creation operator for a particle in a state labeled by n_p and a hole in state n_h, with their angular momenta coupled to J. For charge-exchange transitions between 0^+ analog states, Eq. (5) reduces to

$$Z_0(n,n) = (2j_n+1)^{-1/2}(2T_>)^{-1/2} \times \sum_m |C_m|^2 [T_{mn}(T_{mn}+1) - T_{mn}^z(T_{mn}^z-1)] \quad (6)$$

in an independent-particle representation where

$$|\Phi_I\rangle = \sum_m C_m \Big| \prod_n \phi_n \Big\rangle_m ,$$

$T_>$ is the isospin of the analog states, ϕ_n is a single-particle orbit with quantum numbers labeled by n (e.g., its angular momentum j_n), m labels the occupation numbers for the orbits and the couplings required to complete the specification of a particular term in the target wave function, and T_{mn} is the combined isospin of the nucleons in the nth orbit for the mth term. For the present analysis, the ground state of ^{120}Sn has been represented by a wave function based on average occupation probabilities derived from a BCS model of ^{119}Sn and ^{121}Sn.[42] The average probabilities have been normalized to correspond to 20 excess neutrons. Elementary shell-model configurations have been assumed for the other targets: $(1f_{7/2})^8$, $0.8(1g_{9/2})^{10}+0.6(1g_{9/2})^8(2p_{1/2})^2$, and $(1h_{9/2})^{10}(2f_{7/2})^8(1i_{13/2})^{14}(3p_{3/2})^4(2f_{5/2})^6(3p_{1/2})^2$ for the excess neutrons in ^{48}Ca, ^{90}Zr, and ^{208}Pb, respectively. The single-particle wave functions have been calculated in a potential of the form

$$U(r)=U_0 f(r)+U_{so}\chi^2\frac{1}{r}\frac{d}{dr}f(r)\vec{l}\cdot\vec{\sigma}, \tag{7}$$

where

$$f(r)=\left[1+\exp\left(\frac{r-r_0A^{1/3}}{a_0}\right)\right]^{-1};$$

$$\vec{l}\cdot\vec{\sigma}=j(j+1)-l(l+1)-s(s+1);$$

$r_0=1.3$ fm; $a_0=0.7$ fm; $\chi^2=2.0$ fm^2; $U_{so}=6$ MeV; A is the mass number of the target; l, s, and j are the orbital, spin, and total angular momentum quantum numbers, respectively, of the bound nucleon; and U_0 has been adjusted to reproduce the observed binding energies—except for the unbound IAS protons in ^{90}Nb, ^{120}Sb, and ^{208}Bi, which DWBA70 treats as bound by 0.01 MeV. Coker and Hoffmann have shown that the microscopic form factor for ^{91}Zr, $(p,n)^{91}$Nb(IAS) is essentially unaffected by the decay of the final state and that there is at most a 10% enhancement for ^{209}Bi(p,n)-^{209}Po(IAS).[43] The binding energy of a target neutron in a particular orbit has been obtained by adding the separation energy of the least-bound neutron to the excitation energy of the corresponding neutron-hole state in the isotope of the target element with mass number $A-1$. The differences between the binding energies of protons and neutrons in analog orbits have been taken to be the following (p,n) IAS reaction Q values: -7.175,[44] -12.03,[45] -13.41,[45] and -18.82 MeV[46] for targets of ^{48}Ca, ^{90}Zr, ^{120}Sn, and ^{208}Pb, respectively. The proton and neutron distorted waves have been generated with the Coulomb-corrected ($V_{CC}=0.84$) optical-model potentials of Becchetti and Greenlees[7] (except for the use of the Fu-Perey potential[47] for the approximately 6-MeV neutrons from the analog of ^{208}Pb at $E_p=25$ MeV). Recent calculations[48] of the nucleon-nucleus optical potential indicate that its real part is not nearly as nonlocal as is usually assumed from the phenomenological results of Perey and Buck. Thus, we have not included any corrections for optical-model nonlocality in the present calculations.

The dashed curves in Fig. 3 result from phenomenological nucleon-nucleon forces consistent with Austin's analysis.[15] In particular, the effective interaction has been taken to have the form given by Eq. (4), with a 1.0-fm Yukawa radial dependence and $V_0=-27$ MeV, $V_\sigma=V_{\sigma\tau}=12$ MeV, and $V_\tau=12$ and 18 MeV. The solid curves have been calculated with a realistic force derived from the Reid soft-core nucleon-nucleon potential[49] by Bertsch,[50] who employed the method of Barrett, Hewitt, and McCarthy[51] to solve for the corresponding G matrix in a harmonic-oscillator basis. For compatability with DWBA70, a superposition of four Yukawa potentials (with ranges of 0.2, 0.4, 0.5, and 0.7 fm) has been determined by fitting harmonic-oscillator matrix elements to the original G matrix.[52] Only the central-force terms which act in states of even relative angular momentum have been retained for the present calculations, since the central interaction in odd states appears to be much weaker.[12,52]

Numerical accuracy has been checked by repeating calculations for several choices of matching radius, integration step size, and number of partial waves. Also, comparisons have been made between DWBA70 and DWUCK.[53] Direct-amplitude total cross sections of 7.76 and 7.73 mb for ^{48}Ca$(p,n)^{48}$Sc(IAS) at $E_p=35$ MeV have been calculated with DWBA70 and DWUCK, respectively, using a 1.0-fm Yukawa force with $V_\tau=18$ MeV.

B. Results

Both the phenomenological and realistic forces yield angular distributions which follow the data but are somewhat smoother. The similarity in shape of the dashed and solid curves in Fig. 3 results from the almost perfect spatial overlap of the target ground state and its isobaric analog coupled with the $0^+\rightarrow 0^+$ IAS transitions being dominated by the monopole component of $V_\tau g_\tau(r_{ip})$. The high degree of spatial overlap insures the insensitivity of the (p,n) IAS form factor to details of the initial and final nuclear wave functions and the shape of the nucleon-nucleon interaction. Sensitivity to the latter is further diminished by the similarity of the low multipole components of reasonable forces.[12] Thus, we are not surprised to discover that the total cross sections (σ_T) for these $0^+(p,n)$ IAS reactions depend on the isospin-

flip interaction almost exclusively through its volume integral. For example, the total cross section measured for $^{90}Zr(p,n)^{90}Nb(IAS)$ at E_p = 45 MeV may be reproduced with phenomenological Yukawa interactions of 179 or 180 MeV fm^3 for ranges of 1.0 or 1.4 fm, respectively. The insensitivity to nuclear wave functions has also been tested by varying the independent-particle potentials and configurations. The present study uses a Woods-Saxon potential with essentially the same geometry as employed by Ross, Mark, and Lawson.[54] Calculations with this geometry (r_0 = 1.3 fm and a_0 = 0.7 fm) need a V_T only 2½% greater than that required with r_0 = 1.25 fm and a_0 = 0.65 fm to yield the total cross section observed for $^{48}Ca(p,n)^{48}Sc(IAS)$ at E_p = 35 MeV. Similarly, the most elementary shell-model configuration $[(1g_{7/2})^8(2d_{5/2})^6(2d_{3/2})^4(3s_{1/2})^2]$ gives the same σ_T as the five-orbit BCS wavefunction for $^{120}Sn(p,n)$-$^{120}Sb(IAS)$ at E_p = 25 MeV, if V_T is increased merely ½%.

The effects of noncentral nucleon-nucleon forces have also been investigated. The complete G-matrix interaction[50,52] (including tensor and spin-orbit terms) yields very nearly the same angular distribution for $^{90}Zr(p,n)^{90}Nb(IAS)$ at E_p = 45 MeV as that obtained with the central part alone. As for the tests described in the previous paragraph, the principal difference occurs in the differential cross sections at 0°. However, the total cross section again remains almost constant, decreasing by less than 1% with the inclusion of the noncentral forces.

Figure 4 displays the results of the phenomenological analysis with the 1.0-fm Yukawa nucleon-nucleon interaction. The individual values of V_T have been determined by requiring the calculations to reproduce the corresponding (p,n) IAS total cross sections measured in the present work. The error bars represent the uncertainties due to the σ_T errors listed in Table I. The average values of V_T for proton bombarding energies of 25, 35, and 45 MeV are given in Table II, along with the uncertainties contributed by the errors in the individual values, the root-mean-square (rms) deviations of the individual values, and the combined uncertainties from both of these sources. A noteworthy aspect of the present phenomenological analysis is the absence of any necessity for an appreciable energy dependence of V_T. The average values of $V_T(E_p)$ yield slopes of -0.17 ± 0.21 and -0.07 ± 0.15 for the ranges 25–35 and 35–45 MeV, respectively. There is also no significant A dependence of V_T. Furthermore, the individual values exhibit decreasing dispersion as the bombarding energy increases, which is dramatically reflected by the rms deviations.

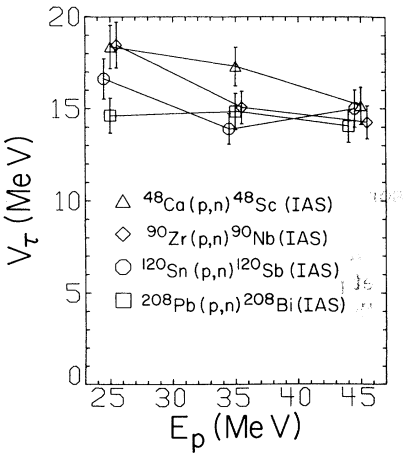

FIG. 4. Phenomenological strengths of effective nucleon-nucleon potentials of the form $V_T(\vec{\tau}_i \cdot \vec{\tau}_p)\exp(-r)/r$ which reproduce the (p,n) IAS total cross sections measured in this work (Table I). For clarity, some points have been slightly displaced in E_p.

The principal source of the observed spread in the individual phenomenological values of V_T for the lower bombarding energies may be uncertainties in the optical-model potentials. In particular, the imaginary terms are smooth functions of projectile energy and target mass in the Becchetti-Greenlees parametrization[7] and may not adequately represent the dependence of the absorption on the target structure.[48] Such effects are more important at lower projectile energies where the number and nature of the open channels are more characteristic of the target.[55] For most (p,n) IAS distorted-wave calculations the least well-established part of the optical model is the neutron imaginary potential, since the neutrons have both lower energies than the protons and inferior elastic scattering data. Fluctuations of almost a factor of 2 in the strength of the imaginary potential have been observed for 8-MeV neutrons scattered from targets with $50 < A < 70$.[56] Thus,

TABLE II. Averages ($\langle V_T \rangle$), uncertainties contributed by the errors in the individual values (ϵ), rms deviations (Δ), and total uncertainties $(\epsilon^2+\Delta^2)^{1/2}$ of the effective nucleon-nucleon potential strengths in Fig. 4.

E_p (MeV)	$\langle V_T \rangle$ (MeV)	ϵ (MeV)	Δ (MeV)	$(\epsilon^2+\Delta^2)^{1/2}$ (MeV)
25	17.0	±0.6	1.6	±1.7
35	15.3	±0.5	1.2	±1.3
45	14.6	±0.5	0.5	±0.7
Over-all Average	15.6	±0.3	1.2	±1.2

we have taken advantage of the Fu-Perey potential, which has been derived from 1–15-MeV neutron cross section data for lead,[47] to describe the distortion of the lowest-energy neutrons of interest in the present study [from ^{208}Pb(p,n)-^{208}Bi(IAS) at $E_p = 25$ MeV]. Unfortunately, such particularly appropriate potentials are not generally available. However, the smooth parametrization of the global potentials is probably adequate at our highest bombarding energy. Calculations with Fu-Perey neutron potentials yield values of V_τ 23%, 14%, and 3% smaller for ^{208}Pb(p,n)-^{208}Bi(IAS) at $E_p = 25$, 35, and 45 MeV, respectively, than the corresponding results with Becchetti-Greenlees potentials. The large disparity at 25 MeV is obviously due to differences in absorption. We have not been the first to notice that (p,n) IAS total cross sections are approximately inversely proportional to the strength of the imaginary potential in the neutron channel.[57]

C. Comparison with other work

Our individual phenomenological values of V_τ cut a relatively narrow swath through the published results of analogous studies for proton bombarding energies up to 50 MeV. We will restrict comparisons to analyses of 0^+ (p,n) IAS reactions induced by protons with energies greater than 20 MeV, since it has been shown that transitions through collective multipole resonances may interfere significantly with the direct amplitude at lower energies.[58] Furthermore, we will only consider calculations employing a real local nucleon-nucleon interaction in a manner consistent with the single inelastic scattering approximation [Eq. (2)]. The quoted values of V_τ will be corrected to the corresponding results for calculations using 1.0-fm Yukawa nucleon-nucleon potentials and including knock-on exchange amplitudes. The corrections for potential shape consist of matching volume integrals, and the exchange corrections are based on our empirical observations that

$$\frac{\sigma_T'}{\sigma_T} \approx \left(\frac{V_\tau'}{V_\tau}\right)^{1.78} \tag{8}$$

and

$$\frac{\sigma_T}{\sigma_T(\text{direct})} \approx (1.7\times10^{-4}E_p - 2.75\times10^{-2})V_\tau - 5\times10^{-3}E_p + 1.955 \tag{9}$$

for the 1.0-fm Yukawa calculations shown in Fig. 3. Without exchange, of course, $\sigma_T \propto V_\tau^2$.

Although they prefer their results which include $(p,d)(d,n)$ contributions, Rickertsen and Kunz[18] and Fielding *et al.*[59] also quote values corresponding to $12.2 \leq V_\tau \leq 18.8$ MeV for one-step fits to (p,n) IAS angular distributions obtained at the University of Colorado from targets with $40 \leq A \leq 96$ at $E_p = 22.8$ MeV. Their phenomenological V_τ's are somewhat more dispersed than ours at $E_p = 25$ MeV, perhaps due to their fitting of differential rather than total cross sections and their use of average proton optical potentials plus symmetry terms for the neutrons coupled with the inclusion of targets farther removed from closed shells. They also fit ^{90}Zr$(p,n)^{90}$Nb(IAS) data acquired with the old Michigan State University neutron time-of-flight system at $E_p = 22$, 30, and 40 MeV[22] and have obtained values corresponding to $V_\tau = 31.3$, 17.4, and 14.1 MeV, respectively. We do not understand their very large value of V_τ at $E_p = 22$ MeV and are more inclined to accept a V_τ of 18.8 MeV derived from an analysis of the same data by Hoffmann and Coker.[60]

The latter authors advocate the use of a complex nucleon-nucleon interaction, the imaginary part of which is claimed to represent the (p,d) (d,n) process. When the imaginary term is included, they indicate little change in the (p,n) IAS total cross sections calculated for ^{90}Zr at $E_p = 22$ to 40 MeV.[60] However, they find it necessary to decrease V_τ from the equivalent of 25.6 MeV (for the real interaction) to 12.6 MeV (with the imaginary term) to reproduce the magnitudes of ^{208}Pb$(p,n)^{208}$Bi(IAS) angular distributions taken at bombarding energies between 24.8 and 50.0 MeV.[61] In contrast, Rickertsen and Kunz report that V_τ must be *increased* by approximately a factor of 2 to compensate for the destructive interference between the direct and $(p,d)(d,n)$ amplitudes.[18] As for the direct calculation of Rickertsen and Kunz for ^{90}Zr$(p,n)^{90}$Nb(IAS) at $E_p = 22$ MeV, we are unable to reproduce the real-interaction calculations of Hoffmann and Coker for ^{208}Pb$(p,n)^{208}$Bi(IAS),[61] which also incorporate an unaccountably large V_τ to fit data consistent with ours (except at $E_p = 25$ MeV).

The present results are in better agreement with the isospin-flip strength corresponding to $V_\tau = 12.2$ MeV obtained by Batty *et al.* for ^{54}Fe(p,n)-^{54}Co(IAS) at $E_p = 30.2$ MeV.[20] Due mostly to an apparent inconsistency in their criteria for fitting the data, they report a 35% smaller V_τ for ^{56}Fe.

To our knowledge, the only other determinations of phenomenological isospin-flip strengths for the effective nucleon-nucleon interaction, within the limitations set forth at the beginnning of this section, are contained in the study of (p,n) reactions on $1p$-shell nuclei by Clough *et al.*[21] They quote average values corresponding to $V_\tau = 25.2 \pm 2.0$ and 9.0 ± 1.1 MeV for incident proton energies of 30 and 50 MeV, respectively. These values of

$V_\tau(E_p)$ yield a slope of -0.81 ± 0.11, suggesting an energy dependence quite inconsistent with the present results. However, considerable sensitivity to the choice of optical-model potentials is noted by these authors, especially for the 30-MeV calculations, and their data are of relatively poor quality by current standards.

The G-matrix interaction produces nearly the same cross sections for the reactions investigated in this work as a 1.0-fm Yukawa potential with $V_\tau = 14$ MeV. Thus, it accounts for the σ_T data quite well at $E_p = 45$ MeV and fairly well at 35 MeV. However, the experimental cross sections at 25 MeV are generally larger than predicted, except for ^{208}Pb$(p,n)^{208}$Bi(IAS), where a particularly appropriate neutron optical potential has been used. Satchler and his collaborators have had reasonable success with microscopic direct-reaction calculations employing another realistic effective interaction,[12,62] the long-range even-state part of the Hamada-Johnston nucleon-nucleon potential.[63] The volume integral of the isospin-flip component of this potential is about 160 MeV fm^3, which corresponds to a 1.0-fm Yukawa potential with $V_\tau = 13$ MeV, not much lower than either our over-all average phenomenological V_τ (15.6 ± 1.2 MeV) or the monopole charge-exchange strength of the G matrix for the Reid soft-core potential.

IV. CONCLUSIONS

Nucleon-induced charge-exchange transitions between 0^+ isobaric-analog states provide an exceptional testing ground for microscopic direct-reaction calculations. The direct cross sections are large, minimizing the relative importance of higher-order processes; the monopole part of the isospin-flip term is the only central-force component of the nucleon-nucleon interaction which contributes to the direct scattering amplitude; the final-state nuclear wave function is essentially the same as for the target ground state; large core-polarization corrections[64] are unnecessary; and suitable optical-model potentials are relatively well established. However, for the microscopic description to remain simple, it is necessary to have sufficient bombarding energy ($E_p \gtrsim 25$ MeV) so that two-step transitions through the giant multipole resonances are negligible.[58]

Unfortunately, the difficulties associated with the detection and energy measurement of very fast neutrons[65] do not currently allow the acquisition of charged-particle quality data with comparable ease. However, with the present time-of-flight system, it has been possible to obtain reasonably complete and accurate angular distributions for charge-exchange reactions induced by protons with energies from 25 to 45 MeV.

We have compared our measured (p,n) IAS cross sections for targets of ^{48}Ca, ^{90}Zr, ^{120}Sn, and ^{208}Pb at $E_p = 25$, 35, and 45 MeV with single inelastic scattering-approximation predictions (including the knock-on exchange amplitudes) based on both phenomenological and realistic effective nucleon-nucleon interactions. We find that the total cross sections for (p,n) reactions to 0^+ isobaric-analog states are mainly sensitive to the volume integral of the isospin-flip central-force component of the effective nucleon-nucleon potential, for which a value of 195 ± 15 MeV fm^3 has been derived from the phenomenological analysis of our data. This is equivalent to a 1.0-fm Yukawa potential with $V_\tau = 15.6 \pm 1.2$ MeV, which suggests that V_τ is now determined at least as well as V_0 and $V_{\sigma\tau}$, and better than V_σ, for $25 \leq E_p \leq 45$ MeV.[15] Although the present results are consistent with no energy dependence of the isospin-flip strength, they lean toward a slight decrease in V_τ as E_p increases over this range. It is reassuring that the individual values of V_τ for ^{208}Pb$(p,n)^{208}$Bi(IAS) exhibit the least fluctuation with bombarding energy, since the most appropriate neutron optical potentials are available for this case, and that the individual values for each target approach the monopole isospin-flip strengths of the long-range part of the Hamada-Johnston potential[12,62] and the G matrix for the Reid soft-core potential[50,52] as E_p increases.

We believe that the instances of apparent disagreement between the present results and those of previous studies of the same type (after corrections are made for antisymmetrization and alternative shapes of the nucleon-nucleon potentials) are mostly due to differences in the choice of optical potentials (mainly the imaginary strength in the neutron channel), the quality of the data, and the criteria employed for comparing theoretical predictions with experimental measurements. In two cases, however, we have been unable to verify previously published calculations of direct (p,n) IAS cross sections, both of which incorporate anomalously large values of V_τ. One of these reported calculations implies that V_τ needs to be *decreased* by almost a factor of 2 when an imaginary interaction representing the $(p,d)(d,n)$ process is included for ^{208}Pb$(p,n)^{208}$Bi(IAS),[61] whereas the same authors indicate that little, if any, change in V_τ is necessary between the corresponding calculations for ^{90}Zr$(p,n)^{90}$Nb(IAS).[60] Both of these results disagree with those of Rickertsen and Kunz, who find that V_τ must be *increased* by approximately a factor of 2 when $(p,d)(d,n)$ is explicitly included via a coupled-

channel Born approximation,[18] except for ^{90}Zr(p,n)-^{90}Nb(IAS) at $E_p = 22$ MeV, for which their single-channel calculation of the direct cross section does not agree with that of Hoffmann and Coker[60] and is also the other case which we have not been able to reproduce.

In addition to the aforementioned disagreement over values of V_T required for (p,n) IAS reactions when $(p,d)(d,n)$ amplitudes are included, recent calculations allowing continuum intermediate states for the deuteron use $V_T \approx 40$ MeV for a 1.0-fm Yukawa potential.[66] Thus, it appears that the actual contributions of such higher-order processes are not yet fully understood. Nevertheless, it is encouraging that for straightforward single inelastic scattering-approximation calculations the isospin-flip strengths of realistic effective nucleon-nucleon interactions are generally consistent with our (p,n) IAS total cross sections, especially at the higher bombarding energies.

---

*Work supported by the National Science Foundation and the Office of Naval Research.

†Present address: Fusion Research Center, University of Texas, Austin, Texas 78712.

[1]K. M. Watson, Phys. Rev. 105, 1388 (1957).
[2]H. A. Bethe, Annu. Rev. Nucl. Sci. 21, 93 (1971); K. A. Brueckner, C. A. Levinson, and H. M. Mahmoud, Phys. Rev. 95, 217 (1954).
[3]F. A. McDonald and M. H. Hull, Jr., Phys. Rev. 143, 838 (1966).
[4]L. S. Rodberg and R. M. Thaler, *Introduction to the Quantum Theory of Scattering* (Academic, New York, 1967).
[5]M. L. Goldberger and K. M. Watson, *Collision Theory* (Wiley, New York, 1964).
[6]N. Austern, *Direct Nuclear Reaction Theories* (Wiley, New York, 1970).
[7]F. D. Becchetti, Jr., and G. W. Greenlees, Phys. Rev. 182, 1190 (1969).
[8]A. K. Kerman, H. McManus, and R. M. Thaler, Ann. Phys. (N.Y.) 8, 551 (1959).
[9]B. R. Barrett and M. W. Kirson, in *Advances in Nuclear Physics*, edited by M. Baranger and E. Vogt (Plenum, New York, 1973), Vol. 6.
[10]F. Petrovich, Ph.D. thesis, Michigan State University, 1970 (unpublished); F. Petrovich, H. McManus, V. A. Madsen, and J. Atkinson, Phys. Rev. Lett. 22, 895 (1969).
[11]B. R. Barrett, in *The Two-Body Force in Nuclei*, edited by S. M. Austin and G. M. Crawley (Plenum, New York, 1972).
[12]W. G. Love and G. R. Satchler, Nucl. Phys. A159, 1 (1970).
[13]D. Slanina and H. McManus, Nucl. Phys. A116, 271 (1968).
[14]G. R. Satchler, Nucl. Phys. A95, 1 (1967).
[15]S. M. Austin, in *The Two-Body Force in Nuclei* (see Ref. 11).
[16]R. A. Hinrichs and D. L. Show, Phys. Rev. C 6, 1257 (1972); W. L. Fadner, J. J. Kraushaar, and S. I. Hayakawa, *ibid.* 859 (1972).
[17]N. B. deTakacsy, Phys. Lett. 42B, 1 (1972).
[18]L. D. Rickertsen and P. D. Kunz, Phys. Lett. 47B, 11 (1973).
[19]R. Schaeffer and G. F. Bertsch, Phys. Lett. 38B, 159 (1972).
[20]C. J. Batty, B. E. Bonner, E. Friedman, C. Tschalar, L. E. Williams, A. S. Clough, and J. B. Hunt, Nucl. Phys. A116, 643 (1968).
[21]A. S. Clough, C. J. Batty, B. E. Bonner, and L. E. Williams, Nucl. Phys. A143, 385 (1970).
[22]R. K. Jolly, T. M. Amos, A. Galonsky, R. Hinrichs, and R. St.Onge, Phys. Rev. C 7, 1903 (1973).
[23]A. Langsford, P. H. Bowen, G. C. Cox, and M. J. M. Saltmarsh, Nucl. Phys. A113, 433 (1968); L. Valentin, *ibid.* 62, 81 (1965).
[24]R. A. Winyard, J. E. Lutkin, and G. W. McBeth, Nucl. Instrum. Methods 95, 141 (1971).
[25]K. Alexander and F. Goulding, Nucl. Instrum. Methods 13, 244 (1961).
[26]R. R. Doering, Michigan State University Cyclotron Laboratory computer program, 1973 (unpublished).
[27]A. M. Lane, in *Isospin in Nuclear Physics*, edited by D. H. Wilkinson (North-Holland, Amsterdam, 1969).
[28]R. Kurz, University of California Report No. UCRL-11339, 1964 (unpublished).
[29]J. C. Hopkins and G. Breit, Nucl. Data A9, 137 (1971).
[30]V. V. Verbinski, W. R. Burrus, T. A. Love, W. Zobel, and N. W. Hill, Nucl. Instrum. Methods 65, 8 (1968).
[31]C. M. Davisson, in *Alpha-, Beta-, and Gamma-Ray Spectroscopy*, edited by K. Siegbahn (North-Holland, Amsterdam, 1965), Vol. 1.
[32]P. R. Bevington, *Data Reduction and Error Analysis for the Physical Sciences* (McGraw-Hill, New York, 1969).
[33]G. F. Bertsch and A. Mekjian, Annu. Rev. Nucl. Sci. 22, 25 (1972).
[34]C. H. Johnson and R. L. Kernell, Oak Ridge National Laboratory Physics Division Annual Progress Report No. ORNL-3778, 1965 (unpublished).
[35]E. C. Booth and B. S. Madsen, Nucl. Phys. A206, 293 (1973).
[36]S. T. Thornton and J. R. Smith, Nucl. Instrum. Methods 96, 551 (1971).
[37]I. E. McCarthy, *Introduction to Nuclear Theory* (Wiley, New York, 1968).
[38]R. Schaeffer, Center for Nuclear Studies of Saclay Report No. CEA-R-4000, 1970 (unpublished).
[39]J. Raynal, Nucl. Phys. A97, 572 (1967).
[40]G. Takeda and K. M. Watson, Phys. Rev. 97, 1336 (1955).
[41]V. A. Madsen, Nucl. Phys. 80, 177 (1966).
[42]V. Gillet, B. Giraud, and M. Rho, Nucl. Phys. A103, 257 (1967).
[43]W. R. Coker and G. W. Hoffmann, Phys. Lett. 40B, 81 (1972).

[44]J. Rapaport, Nucl. Data B4, 351 (1970).
[45]J. D. Carlson, Ph.D. thesis, University of Colorado, 1972 (unpublished).
[46]G. M. Crawley, P. S. Miller, A. Galonsky, T. Amos, and R. Doering, Phys. Rev. C 6, 1890 (1972).
[47]C. Y. Fu and F. G. Perey, Oak Ridge National Laboratory Report No. ORNL-4765, 1972 (unpublished).
[48]C. L. Rao, M. Reeves, III, and G. R. Satchler, Nucl. Phys. A207, 182 (1973).
[49]R. Reid, Ann. Phys. (N.Y.) 50, 411 (1968).
[50]G. F. Bertsch, *The Practitioner's Shell Model* (North-Holland, Amsterdam, 1972).
[51]B. R. Barrett, R. G. L. Hewitt, and R. J. McCarthy, Phys. Rev. C 3, 1137 (1971).
[52]J. Borysowicz, H. McManus, and G. Bertsch, Michigan State University Cyclotron Laboratory Report, 1974 (unpublished).
[53]P. D. Kunz, University of Colorado computer program, 1972 (unpublished).
[54]A. Ross, H. Mark, and R. D. Lawson, Phys. Rev. 104, 401 (1956).
[55]T. F. O'Dwyer, M. Kawai, and G. E. Brown, Phys. Lett. 41B, 259 (1972).
[56]B. Holmquist and T. Wiedling, Nucl. Phys. A188, 24 (1972).
[57]G. T. Garvey and P. S. Miller, Phys. Lett. 28B, 243 (1968); G. R. Satchler, R. M. Drisko, and R. H. Bassel, Phys. Rev. 136, B637 (1964).
[58]K. A. Amos and H. V. Geramb, Z. Phys. 270, 149 (1974).
[59]H. W. Fielding, L. D. Rickertsen, P. D. Kunz, D. A. Lind, and C. D. Zafiratos, Phys. Rev. Lett. 33, 226 (1974).
[60]G. W. Hoffmann and W. R. Coker, Z. Phys. 269, 307 (1974).
[61]G. W. Hoffmann and W. R. Coker, Phys. Lett. 47B, 285 (1973).
[62]G. R. Satchler, Z. Phys. 260, 209 (1973).
[63]T. Hamada and I. D. Johnston, Nucl. Phys. 34, 382 (1962).
[64]H. McManus, in *The Two-Body Force in Nuclei* (see Ref. 11).
[65]P. Marmier and E. Sheldon, *Physics of Nuclei and Particles* (Academic, New York, 1970), Vol. 2.
[66]P. D. Kunz and L. D. Rickertsen, University of Colorado Technical Progress Report No. COO-535-710, 1974 (unpublished); and private communication.